HHS Public Access

Author manuscript

Pharm Res. Author manuscript; available in PMC 2020 August 13.

Published in final edited form as:

Pharm Res. ; 35(8): 164. doi:10.1007/s11095-018-2444-z.

Local Application of Pyrophosphorylated Simvastatin Prevents Experimental Periodontitis

Xiaobei Wang[1,#], **Zhenshan Jia**[1,#], **Yosif Almoshari**[1,2,#], **Subodh M. Lele**[3], **Richard A. Reinhardt**[4], **Dong Wang**[1,*]

[1]The Department of Pharmaceutical Sciences, College of Pharmacy, University of Nebraska Medical Center, Omaha, NE, 68198, USA.

[2]The Department of Pharmaceutics, College of Pharmacy, Jazan University, Jazan 45142, Saudi Arabia.

[3]The Department of Pathology & Microbiology, College of Medicine, University of Nebraska Medical Center, Omaha, NE 6819, USA.

[4]The Department of Surgical Specialties, College of Dentistry, University of Nebraska Medical Center, Lincoln, NE 68583, USA.

Abstract

Purpose.—Simvastatin (SIM), a HMG-CoA reductase inhibitor widely prescribed for hypercholesterolemia, has been reported to ameliorate inflammation and promote osteogenesis. Its clinical applications on these potential secondary indications, however, have been hampered by its lack of osteotropicity and poor water solubility. To address this challenge, we propose to design and evaluate the therapeutic efficacy of a novel simvastatin prodrug with better water solubility and bone affinity.

Method.—The prodrug (SIM-PPi) was synthesized by directly conjugating a SIM trimer to a pyrophosphate (PPi). It was characterized and evaluated *in vitro* for its water solubility, osteotropicity, toxicity, anti-inflammatory and osteoinductive properties. It was then tested for anti-inflammatory and osteoinductive properties *in vivo* by three weekly injections into gingiva of a ligature-induced experimental periodontitis rat model.

Results.—*In vitro* studies showed that SIM-PPi has greatly improved water-solubility of SIM and shows strong binding to hydroxyapatite (HA). In macrophage culture, SIM-PPi inhibited LPS-induced pro-inflammatory cytokines (IL-1β, IL-6). In osteoblast culture, it was found to significantly increase alkaline phosphatase (ALP) activity with accelerated mineral deposition, confirming the osteogenic potential of SIM-PPi. When tested *in vivo* on an experimental periodontal bone-loss model, SIM-PPi exhibited a superior prophylactic effect compared to dose equivalent SIM in reducing inflammatory cells and in preserving alveolar bone structure, as shown in the histological and micro-CT data.

[*]Corresponding author. (986125 Nebraska Medical Center, PDD 3020, Omaha, Nebraska 68198-6125, USA. dwang@unmc.edu, Tel.: +1-402-559-1995, Fax: +1-402-559-9543).

[#]These authors contributed equally to this work.

Conclusion.—SIM-PPi may have the potential to be further developed for better clinical management of bone loss associated with periodontitis.

Keywords

Periodontitis; Simvastatin; Pyrophosphate; Prodrug; Periodontal bone loss

INTRODUCTION

Periodontitis is an oral inflammatory disease that affects the integrity of tooth-supporting tissues including gingiva, periodontal ligament, cementum, and alveolar bone. The pathogenic bacterial population and host immune response are considered as keystones in the emergence and persistence of the disease(1). The disease afflicts 45.9 % of adults in the United States, confirming the high burden of periodontitis(2). The harmful health impact of periodontitis is not only limited to the local tissue destruction and alveolar bone resorption, but it may also affect systemic health by increasing the incidence risk of systemic inflammatory diseases, atherosclerosis, and cancer(3). Non-surgical treatment options are limited to plaque (biofilm) removal which aim to reduce inflammation(4) followed by administration of local and systemic antibiotics to minimize bacterial load in the periodontal pocket(5,6). Additionally, nonsteroidal anti-inflammatory medications, sub-antimicrobial doses of doxycycline, and growth factors have all been utilized as host modulation agents to reduce disease progression(7,8). However, their effect on the inflammation-induced alveolar bone loss is limited. Hence, there is an urgent need for the development of a medication that can prevent/regenerate alveolar bone loss.

Statins are a class of anti-hyperlipidemic agents which act mainly through hepatic 3-hydroxy-3-methylglutaryl (HMG)-CoA reductase inhibition, thereby affecting the metabolic pathway that produces cholesterol(9). Researchers have found that statins, such as simvastatin (SIM) and lovastatin, induce the expression of bone morphogenic protein-2 (BMP-2) leading to substantial osteogenic effects(10,11). Furthermore, SIM has been reported as a potent antimicrobial agent against both *A. actinomycetemcomitans* and *P. gingivalis*(12), and an anti-inflammatory agent that reduces the expression of cytokines such as IL-6, IL-8, and MCP-1, both *in vitro* and *in vivo* by inhibiting the activation of NF-κB that regulates the expression of diverse inflammatory cytokines(13,14). Due to these unique therapeutic properties, statins have been considered as potential therapeutic candidates for inflammatory diseases and skeletal disorders. The translation of this therapeutic potential into clinical practice, however, has been largely hampered by the statins' lack of tissue specificity, especially to the bone.

Systemic administration of SIM has been investigated for effects on periodontitis-associated alveolar bone loss and has exhibited a limited impact on periodontal bone due to its hepatotropicity resulting in very limited drug concentration at the skeletal tissues(15). However, local delivery of simvastatin suspended in gel as an adjunct to mechanical periodontal treatment (scaling and root planing) has been shown to improve bone regeneration in chronic(16,17) and aggressive periodontitis(18). Meta-analysis has

confirmed simvastatin as an effective adjunct to scaling and root planing for creating bone fill(19).

Local delivery systems of SIM have been developed to enhance solubility and provide a sustained release, and have shown potential protection of the periodontal tissues(20,21). As a novel strategy to address the limitations associated with the clinical utility of SIM for periodontal disease, we here report the development of a SIM prodrug by conjugating a SIM trimer to osteotropic pyrophosphate (PPi). The prodrug (SIM-PPi) was fully characterized, and its therapeutic efficacy was evaluated *in vitro* and on an experimental periodontitis rat model.

METHODS AND MATERIALS

Materials

Simvastatin was purchased from Zhejiang Ruibang Laboratories (Wenzhou, Zhejiang, China) Hydroxyapatite microparticles (HA, DNA grade Bio-Gel HTP gel) were purchased from Bio-Rad (Hercules, CA, USA). Mouse macrophage Raw 264.7, osteoblast MC3T3-L1 cells, and Dulbecco's Modified Eagle Medium (DMEM) were originally purchased from ATCC (Manassas, VA, USA). Minimum Essential Media (alpha-MEM) and trypsin-EDTA were purchased from Gibco (Grand Island, NY, USA). Fetal bovine serum (FBS) was obtained from Gemini BenchMark (West Sacramento, CA). Silver nitrate was purchased from RICCA Chemical Company (Arlington, TX). Sodium thiosulfate was purchased from Alfa Aesar (Haverhill, MA). All other reagents and solvents, if not specified, were obtained from either Fisher Scientific (Pittsburgh, PA, USA) or Acros Organics (Morris Plains, NJ, USA).

Synthesis of the simvastatin-pyrophosphate prodrug (SIM-PPI)

Synthesis of compound 1—Simvastatin (6.27g, 15 mmol), butane-1,4-diol (27.3g, 300 mmol) and *p*-toluenesulfonic acid monohydrate ($TsOH{\cdot}H_2O$, 285 mg, 1.5mmol) were dissolved in anhydrous CH_2Cl_2 (30 mL). The solution was stirred at room temperature for 3 hr. $NaHCO_3$ (saturated solution, 15 mL) and ethyl acetate (100 mL) were added and then washed with brine (80 mL×3). The organic phase was dried over Na_2SO_4 and then the solvent was removed. The residue was purified by flash column chromatography (ethyl acetate/hexanes = 3/1) to give compound 1 (5.76 g), yield: 75.6%.

^{1}H NMR (500 MHz, $CDCl_3$): δ (ppm) = 5.97 (d, *J* = 9.7 Hz, 1H), 5.78 (dd, *J* = 9.7 Hz, 6.3 Hz, 1H), 5.49 (s, 1H), 5.38 (d, *J* = 2.5 Hz, 1H), 4.26 (d, *J* = 3.8 Hz, 1H), 4.20 (s, 1H), 4.16 (t, *J* = 6.5 Hz, 2H), 3.83 (s, 1H), 3.78 (br, 1H), 3.67 (t, *J* = 6.0 Hz, 2H), 2.49 (s, 1H), 2.48 (s, 1H), 2.43 (m, 1H), 2.39 (s, 1H), 2.36 (dd, *J* = 12.3 Hz, 6.2Hz, 1H), 2.24 (d, *J* = 10.6 Hz, 1H), 1.95 (m, 2H), 1.76 (m, 2H), 1.60–1.70 (m, 4H), 1.45–1.60 (m, 5H), 1.26 (m, 1H), 1.19 (m, 1H), 1.12 (s, 3H), 1.11 (s, 3H), 1.08 (d, *J* = 7.4 Hz, 3H), 0.87 (d, *J* = 7.0 Hz, 3H), 0.83 (t, *J* = 7.5 Hz, 3H).

^{13}C NMR (125 MHz, $CDCl_3$): δ (ppm) = 178.14, 172.27, 133.04, 131.54, 129.45, 128.20, 72.15, 68.95, 68.08, 64.50, 61.96, 42.90, 42.29, 41.94, 37.61, 36.19, 34.74, 32.93, 32.89, 30.42, 28.94, 27.19, 24.98, 24.70, 24.59, 24.14, 23.00, 13.79, 9.21.

MS (ESI): m/z = 531.1 ($M + Na^+$), calculated MW = 508.3.

Synthesis of compound 2—Compound 1 (6.5 g, 12.8 mmol) and imidazole (1.74 g, 25.6 mmol) were dissolved in anhydrous CH_2Cl_2 (30 mL) and cooled to 0 °C. *t*-Butyldimethylsilyl chloride (TBSCl, 2.10 g, 14 mmol) was added. The solution was stirred at 0 °C for 3 hr. Ethyl acetate (100 mL) were added and then washed with brine (80 mL×3). The organic phase was dried over Na_2SO_4 and then the solvent was removed. The residue was purified by flash column chromatography (ethyl acetate/hexanes = 1/1) to give compound 1 (7.18 g), yield: 90.2%.

^{1}H NMR (500 MHz, $CDCl_3$): δ (ppm) = 5.93 (d, *J* = 9.7 Hz, 1H), 5.73 (dd, *J* = 9.7 Hz, 6.3Hz, 1H), 5.44 (s, 1H), 5.34 (d, *J* = 2.6 Hz, 1H), 4.21, (br, 1H), 4.09 (t, *J* = 6.6 Hz, 2H), 4.07 (s, 1H), 3.79, (s, 1H), 3.73 (br, 1H), 3.59 (t, *J* = 6.2 Hz, 2H), 2.44 (s, 1H), 2.43 (s, 1H), 2.39 (m, 1H), 2.33 (dd, *J* = 11.4 Hz, 6.1Hz), 2.19 (d, *J* = 10.6 Hz, 1H), 1.90 (br, 2H), 1.65 (m, 2H), 1.53 (m, 9H), 1.21 (m, 1H), 1.14 (m, 1H), 1.08 (s, 3H), 1.07 (s, 3H), 1.04 (d, *J* = 7.4 Hz, 3H), 0.85 (s, 9H), 0.82 (s, d, *J* = 7.0 Hz, 3H), 0.78 (t, *J* = 7.5 Hz, 3H), 0.01 (s, 6H).

^{13}C NMR (125 MHz, $CDCl_3$): δ (ppm) = 177.81, 172.18, 132.93, 131.50, 129.28, 128.14, 72.02, 68.81, 67.92, 64.47, 62.32, 42.76, 42.27, 41.71, 37.52, 36.13, 34.69, 32.82, 30.34, 28.96, 27.12, 25.76, 25.01, 24.62, 24.51, 24.10, 22.92, 18.10, 13.71, 9.13, −5.50

MS (ESI): m/z = 645.5 ($M + Na^+$), calculated MW = 622.4.

Synthesis of compound 3—Compound 2 (5.35 g, 7 mmol), triethylamine (2.12 g, 3 mmol) and 4-dimethylaminopyridine (DMAP, 170 mg, 1.4 mmol) were dissolved in anhydrous CH_2Cl_2 (20 mL) and cooled to 0 °C. Ac_2O (1.78 g, 17.5 mmol) was added. The solution was stirred at 0 °C for 0.5 hr. Ethyl acetate (70 mL) was added and washed with HCl (25 mL, 1 M) and brine (100 mL). The organic phase was dried over Na_2SO_4 and then the solvent was removed to give crude product compound 3 (4.90 g). It was used directly in the next reaction without further purification.

^{1}H NMR (500 MHz, $CDCl_3$): δ (ppm) = 5.93 (d, *J* = 9.7 Hz, 1H), 5.73 (dd, *J* = 9.7 Hz, 6.3Hz, 1H), 5.45 (s, 1H), 5.30 (d, *J* = 2.6Hz, 1H), 5,19 (pent, *J* = 6.2 Hz), 4.84 (m, 1H), 4.06 (t, *J* = 6.6 Hz, 2H), 3.60 (t, *J* = 6.2 Hz, 2H), 2.57 (s, 1H), 2.56 (s, 1H), 2.39 (m, 1H), 2.33 (dd, *J* = 11.4Hz, 6.1Hz), 2.19 (d, *J* = 11.7 Hz, 1H), 2.02 (s, 3H), 1.96 (s, 3H), 1.93 (m, 3H), 1.82 (m, 1H), 1.60–1.70 (m, 4H), 1.40–1.60 (m, 5H), 1.31 (m, 1H), 1.14 (m, 1H), 1.08 (s, 3H), 1.07 (s, 3H), 1.04 (d, *J* = 7.4 Hz, 3H), 0.85 (s, 9H), 0.82 (d, *J* = 7.0 Hz, 3H), 0.78 (t, *J* = 7.5 Hz, 3H), 0.01 (s, 6H).

^{13}C NMR (125 MHz, $CDCl_3$): δ (ppm) = 177.32, 170.33, 169.87, 169.81, 132.68, 131.41, 129.53, 128.26, 70.95, 67.73, 67.63, 64.51, 62.34, 42.74, 38.58, 37.57, 37.39, 36.25, 32.81, 32.72, 30.99, 30.35, 28.96, 27.14, 25.78, 25.05, 24.59, 24.53, 23.24, 22.89, 21.03, 20.88, 18.14, 13.64, 9.14, −5.48

MS (ESI): m/z = 729.7 ($M + Na^+$), calculated MW = 706.5.

Synthesis of compound 4—Compound 3 (4.90g, 6.9 mmol) was dissolved in a mixture solution (MeOH/CH_2Cl_2 = 1/1, 20 mL) and cooled to 0 °C. TsOH monohydrate (133 mg, 0.7 mmol) was added. The solution was stirred at 0 °C for 1 hr. Ethyl acetate (100 mL) was added and then washed with brine (80 mL×3). The organic phase was dried over Na_2SO_4 and then the solvent was removed. The residue was purified by flash column chromatography (ethyl acetate/hexanes = 1/1) to give compound 4 (3.69 g), yield: 89.0% for two steps.

^{1}H NMR (500 MHz, $CDCl_3$): δ (ppm) = 5.88 (d, *J* = 9.7 Hz, 1H), 5.66 (dd, *J* = 9.7 Hz, 6.3Hz, 1H), 5.40 (s, 1H), 5.23 (d, *J* = 2.6Hz, 1H), 5.13 (pent, *J* = 6.2 Hz), 4.77 (m, 1H), 4.06 (m, 2H), 3.60 (t, *J* = 6.2 Hz, 2H), 2.514 (s, 1H), 2.510 (s, 1H), 2.50 (t, *J* = 3.8 Hz, 1H), 2.33 (m, 1H), 2.26 (dd, *J* = 11.4Hz, 6.1Hz, 1H), 2.19 (d, *J* = 11.7Hz, 1H), 1.96 (s, 3H), 1.93 (s, 3H), 1.86 (m, 3H), 1.76 (m, 1H), 1.45–1.65 (m, 9H), 1.26 (m, 1H), 1.06 (m, 1H), 1.02 (s, 3H), 1.01 (s, 3H), 0.98 (d, *J* = 7.4 Hz, 3H), 0.77 (d, *J* = 7.0 Hz, 3H), 0.73 (t, *J* = 7.5 Hz, 3H).

^{13}C NMR (125 MHz, $CDCl_3$): δ (ppm) = 177.34, 170.38, 169.86, 169.78, 132.54, 131.25, 129.40, 128.13, 70.90, 67.64, 67.59, 64.34, 61.67, 42.63, 38.53, 37.48, 37.23, 36.12, 32.67, 32.56, 30.91, 30.22, 28.74, 27.00, 24.80, 24.46, 24.39, 23.14, 22.76, 20.90, 20.75, 13.50, 9.02

MS (ESI): m/z = 615.4 ($M + Na^+$), calculated MW = 592.4.

Synthesis of compound 5—Compound 2 (2.50 g, 4.0 mmol), succinic anhydride (1.6 g, 16 mmol), triethyl amine (2.0 g, 20 mmol) and DMAP (146 mg, 1.2 mmol) were dissolved in anhydrous CH_2Cl_2 (20 mL). The solution was stirred overnight. Ethyl acetate (70 mL) was added and then washed with HCl (25 mL, 1 M) and brine (100 mL). The organic phase was dried over Na_2SO_4 and then the solvent was removed. The residue was purified by flash column chromatography (ethyl acetate/hexanes = 1/1 and trace amount of acetic acid) to give compound 5 (2.89 g), yield: 87.8%.

^{1}H NMR (500 MHz, $CDCl_3$): δ (ppm) = 10.79 (br, 2H), 5,96 (d, *J* = 9.7 Hz, 1H), 5.75 (dd, *J* = 9.7 Hz, 6.3Hz, 1H), 5.48 (s, 1H), 5.35 (d, *J* = 2.6 Hz, 1H), 5,23 (pent, *J* = 6.2 Hz), 4.89 (m, 1H), 4.08 (t, *J* = 6.6 Hz, 2H), 3.63 (t, *J* = 6.2 Hz, 2H), 2.55–2.75 (m, 10H), 2.42 (s, 1H), 2.34 (dd, *J* = 11.4 Hz, 6.1Hz, 1H), 1.94 (m, 1H), 1.87 (s, 3H), 1.84 (m, 1H), 1.60–1.70 (m, 4H), 1.40–1.60 (m, 5H), 1.34 (m, 1H), 1.105 (s, 3H), 1.098 (s, 3H), 1.06 (d, *J* = 7.4 Hz, 3H), 0.85 (s, 9H), 0.81 (d, *J* = 7.0 Hz, 3H), 0.80 (t, *J* = 7.5 Hz, 3H), 0.05 (s, 6H).

^{13}C NMR (125 MHz, $CDCl_3$): δ (ppm) = 178.11, 177.32, 176.71, 171.66, 171.17, 170.07, 132.79, 131.43, 129.57, 128.26, 71.55, 68.12, 68.04, 64.62, 62.57, 42.92, 38.43, 37.73, 37.47, 36.13, 32.86, 31.10, 30.35, 29.02, 28.93, 28.79, 27.16, 25.85, 25.03, 24.60, 24.58, 23.60, 22.97, 18.23, 13.69, 9.19, −5.42.

MS (ESI): m/z = 845.0 ($M + Na^+$), calculated MW = 822.4.

Synthesis of compound 6—Compound 5 (1.65 g, 2.0 mmol) and DMAP (73 mg, 0.6 mmol) were dissolved in anhydrous CH_2Cl_2 (20 mL) and cooled to 0 °C. *N,N'*-Dicyclohexylcarbodiimide (DCC, 1.24 g, 6.0 mmol) in anhydrous CH_2Cl_2 (5 mL) was

added and then compound 4 (2.48 g, 4.6 mmol) was added. The solution was stirred at 0 °C for 1 hr. Dichloromethane (70 mL) was added and filtered to remove the solid. The filtrate was then concentrated. The residue was purified by column chromatography (ethyl acetate/hexanes = 1/2 to 1/1) to give compound 6 (3.53 g), yield: 89.6%.

^{1}H NMR (500 MHz, $CDCl_3$): δ (ppm) = 5,93 (d, *J* = 9.7 Hz, 3H), 5.73 (dd, *J* = 9.7 Hz, 6.3Hz, 3H), 5.45 (s, 3H), 5.29 (d, *J* = 2.6 Hz, 3H), 5,18 (pent, *J* = 6.1 Hz, 3H), 4.83 (m, 3H), 4.08 (m, 10H), 3.58 (t, *J* = 6.2 Hz, 2H), 2.59 (s, 3H), 2. 56 (m, 14H), 2.34 (dd, *J* = 11.4 Hz, 6.1Hz, 1H), 2.21 (d, *J* = 11.7 Hz, 1H), 2.02 (s, 6H), 1.98 (s, 6H), 1.94 (m, 9H), 1.87 (m, 3H), 1.40–1.70 (m, 27H), 1.31 (m, 3H), 1.14 (m, 3H), 1.07 (s, 9H), 1.06 (s, 9H), 1.03 (d, *J* = 7.4 Hz, 9H), 0.84 (s, 9H), 0.82 (d, *J* = 7.0 Hz, 9H), 0.78 (t, *J* = 7.5 Hz, 9H), 0.01 (s, 6H).

^{13}C NMR (125 MHz, $CDCl_3$): δ (ppm) = 177.28, 177.23, 171.98, 171.85, 171.59, 171.12,, 170.29, 169.78, 169.76, 169.74, 132.68, 132.62, 131.39, 131.36, 129.49, 129.46, 128.21, 71.34, 70.89, 67.91, 67.64, 67.58, 64.46, 63.94, 63.93, 63.87, 63.85, 62.31, 60.12, 42.69, 38.51, 38.29, 37.57, 37.33, 36.20, 32.76, 32.67, 30.96, 30.30, 28.99, 28.92, 28.76, 28.72, 27.09, 25.75, 25.01, 24.55, 24.51, 24.48, 23.40, 23.21, 22.84, 20.99, 20.83, 18.10, 14.02, 13.63, 13.60, 9.11, 05.51

MS (ESI): m/z = 1994.9 ($M + Na^+$), calculated MW = 1971.4.

Synthesis of compound 7—Compound 6 (3.13 g, 1.59 mmol) was dissolved in a mixture solution (methanol/CH_2Cl_2 = 1/1, 20 mL) and cooled to 0 °C. TsOH monohydrate (60.4 mg, 0.32 mmol) was added. The solution was stirred at 0 °C for 1 hr. Ethyl acetate (100 mL) was added and then washed with brine (80 mL×3). The organic phase was dried over Na_2SO_4 and then the solvent was removed. The residue was purified by flash column chromatography (ethyl acetate/hexanes = 1/1) to give compound 7 (2.59 g), yield: 87.8%.

^{1}H NMR (500 MHz, $CDCl_3$): δ (ppm) = 5.97 (d, *J* = 9.7Hz, 3H), 5.77 (dd, *J* = 9.7 Hz, 6.3Hz, 3H), 5.50 (s, 3H), 5.33(d, *J* = 2.6Hz, 3H), 5.23 (pent, *J* = 6.1 Hz, 3H), 4.87 (m, 3H), 4.11 (m, 10H), 3.66 (t, *J* = 6.2 Hz, 2H), 2.61 (m, 14H), 2.43 (s, 3H), 2.34 (dd, *J* = 11.4 Hz, 6.1Hz, 3H), 2.21 (d, *J* = 11.7 Hz, 3H), 2.06 (s, 6H), 2.04 (s, 6H), 1.94 (m, 9H), 1.85 (m, 3H), 1.50–1.70 (m, 24H), 1.46 (m, 3H), 1.33 (m, 3H), 1.13 (m, 3H), 1.11 (s, 9H), 1.10 (s, 9H), 1.07 (d, *J* = 7.4 Hz, 9H), 0.86 (s, 9H), 0.82 (d, *J* = 7.0 Hz, 9H), 0.82 (t,, *J* = 7.4 Hz, 9H).

^{13}C NMR (125 MHz, $CDCl_3$): δ (ppm) = 177.45, 172.15, 172.09, 171.78, 171.26, 170.47, 169.94, 169.84, 177.45, 172.15, 172.09, 171.78, 171.26, 170.47, 169.94, 169.84, 132.74, 131.45, 129.63, 128.30, 71.43, 71.00, 68.08, 67.75, 67.71, 64.50, 64.06, 64.00, 62.07, 42.81, 38.61, 38.47, 37.66, 37.43, 36.29, 32.87, 32.86, 32.76, 31.16, 31.06, 30.40, 29.09, 29.03, 28.86, 28.80, 27.19, 25.09, 24.98, 24.66, 24.64, 24.61, 24.58, 23.54, 23.31, 22.94, 21.10, 20.95, 13.73, 13.69, 9.21, 9.20

MS (ESI): m/z = 1880.6 ($M + Na^+$), calculated MW = 1857.4

Synthesis of compound 8—Compound 7 (386 mg, 0.21 mmol) and DMAP (5.1 mg, 0.04 mmol) were dissolved in anhydrous dichloromethane (20 mL) and cooled to 0 °C. DCC (65g, 0.315mmol) in anhydrous dichloromethane (3 mL) was added and then bromoacetic

acid (38.4 mg, 0.27 mmol) was added. The solution was stirred at 0 °C for 1 hr. Dichloromethane (70 mL) was added and filtered to remove the solid. The filtrate was then concentrated. The residue was purified by column chromatography (ethyl acetate/hexanes = 1/2) to give compound 8 (336 mg, 0.172 mmol), yield: 82.1%.

^{1}H NMR (500 MHz, $CDCl_3$): δ (ppm) = 5.97 (d, *J* = 9.7Hz, 3H), 5.77 (dd, *J* = 9.7Hz, 6.3Hz, 3H), 5.50 (s, 3H), 5.33(d, *J* = 2.6 Hz, 3H), 5.23 (pent, *J* = 6.1 Hz, 3H), 4.87 (m, 3H), 4.20 (t, 5.8 Hz, 2H), 4.11 (m, 10H), 3.85 (s, 2H), 3.65 (t, *J* = 6.2 Hz, 2H), 2.63 (s, 6H), 2.63 (s, 6H), 2.61 (s, 4H), 2.59 (s, 4H), 2.43 (s, 3H), 2.34 (dd, *J* = 11.4 Hz, 6.1 Hz, 3H), 2.22 (d, *J* = 11.7Hz, 3H), 2.06 (s, 6H), 2.04 (s, 6H), 1.94 (m, 9H), 1.85 (m, 3H), 1.50–1.70 (m, 24H), 1.46 (m, 3H), 1.33 (m, 3H), 1.13 (m, 3H), 1.11 (s, 9H), 1.10 (s, 9H), 1.07 (d, *J* = 7.4 Hz, 9H), 0.86 (d, *J* = 7.0Hz, 9H), 0.82 (t,, *J* = 7.4Hz, 9H).

^{13}C NMR (125 MHz, $CDCl_3$): δ (ppm) = 177.39, 177.35, 172.06, 171.94, 171.71, 171.20, 170.40, 169.87, 169.77, 167.07, 132.70, 131.42, 129.59, 128.27, 71.38, 70.96, 67.95, 67.71, 67.67, 65.52, 64.02, 64.00, 63.98, 63.94, 63.89, 42.77, 38.58, 38.35, 37.67, 37.62, 37.40, 36.26, 32.84, 32.82, 32.73, 31.07, 31.02, 30.37, 29.05, 28.98, 28.82, 28.76, 27.15, 25.68, 25.06, 24.95, 24.63, 24.61, 24.58, 24.55, 23.50, 23.28, 22.90, 21.07, 20.91, 13.70, 13.66, 9.16.

Synthesis of compound 9—Compound 8 (300 mg, 0.154 mmol) was dissolved in anhydrous acetonitrile (5 mL) and cooled to 0°C. Tris(tetrabutylammonium) hydrogen pyrophosphate (277 mg, 0.308 mmol) was added. The solution was stirred at 0 °C for 1 hr. The organic solvent was removed. The residue was then dissolved in water and the solution went through the sodium resin to exchange the cation to sodium. The elution was then lyophilized. The residue was then purified by cellulose column chromatography (isopropanol/acetonitrile/H_2O = 1:1:2) to give product compound 9 (176 mg), yield: 54.1%.

^{1}H NMR (500 MHz, DMSO): δ (ppm) = 5.95 (d, *J* = 9.7 Hz, 3H), 5.77 (dd, *J* = 9.7 Hz, 6.3Hz, 3H), 5.50 (s, 3H), 5.2 (s, 3H), 5.11 (pent, *J* = 6.1 Hz, 3H), 4.76 (m, 3H), 4.35 (d, 6.1 Hz, 2H), 4.09 (s, 2H), 4.03 (s, 8H), 2.63 (m, 6H), 2.56 (m, 12H), 2.47 (s, 3H), 2.38 (dd, *J* = 11.4 Hz, 6.1Hz, 3H), 2.24 (d, *J* = 11.7 Hz, 3H), 1.98 (s, 6H), 1.97 (s, 6H), 1.94 (m, 9H), 1.85 (m, 3H), 1.50–1.70 (m, 24H), 1.46 (m, 3H), 1.33 (m, 3H), 1.13 (m, 3H), 1.04 (s, 9H), 1.02 (s, 9H), 1.01 (d, *J* = 7.4 Hz, 9H), 0.81 (d, *J* = 7.0 Hz, 9H), 0.76 (t,, *J* = 7.4Hz, 9H).

^{31}P NMR (202.5MHz, DMSO): δ (ppm) = −9.46, −10.67.

Comparing aqueous solubility of SIM-PPi and SIM

This experiment was conducted to compare the aqueous solubility of SIM-PPi and free SIM. The solubility values of SIM-PPi and SIM were obtained by measuring equilibrium solubility after adding the analyte to the testing medium for a predetermined period of time(22,23). Briefly, SIM-PPi and SIM (1 mg/mL each), were added to either deionized water or phosphate buffer in microcentrifuge tubes. The suspensions were agitated on a rotor at 22 ± 2 °C for 48 hr to reach the equilibrium. The mixtures were then centrifuged (2,000 rpm, 5 min) to settle the undissolved drug. The supernatants (saturated solutions) were obtained by filtering through 0.2 μm syringe filters, and then the SIM-PPi and SIM

concentrations were measured using a UV spectrophotometer (SpectraMax M2, Molecular Devices, Sunnyvale, CA, USA) at 230 nm.

In vitro hydroxyapatite (HA) binding assay

To predict the binding of SIM-PPi to HA, which is the primary inorganic component of natural hard tissues, an *in vitro* binding test was performed using HA particles (Bio-Gel HTP, particle size is a range of 10–90 um, Bio-Rad). Briefly, SIM-PPi (1 mg/mL) was dissolved in 4 mL 25% isopropyl alcohol (1 mL of isopropyl alcohol diluted in 3 mL of 1.3× PBS to achieve final concentration of 1× PBS composed of 11.9 mM phosphates, 137 mM sodium chloride, and 2.7 mM potassium chloride). HA (100 mg) was then added to the solution. The PBS solution of alendronate (ALN) and SIM acid were separately prepared and mixed with HA (100 mg) for the binding analysis. All binding media contained 11.9 mM phosphates, 137 mM sodium chloride, and 2.7 mM potassium chloride. All three suspensions were agitated in micro-centrifuge tubes on a rotary mixer for varying lengths of time (30 min, 2 hr and 6 hr). At the end of each time point, the HA was spun down by centrifuging at 85 ×g for 5 min. The binding affinity was assessed by measuring the relative concentration of SIM-PPi, SIM, and ALN in the supernatants. The concentrations of SIM-PPi and SIM was detected by measuring the absorbance at 230 nm using a UV spectrophotometer (SpectraMax M2, Molecular Devices, Sunnyvale, CA, USA). The concentration of ALN was measured using the ninhydrin assay(24). The relative HA binding was calculated according to the following formula:

$$\text{HA binding}(\%) = \frac{(X - Y)}{X} \times 100$$

where X is the initial concentration (1 mg/mL) and Y is the concentration in the supernatant after incubation with HA.

Cell culture

Cell viability assay—Mouse macrophage Raw 264.7 and osteoblast MC3T3-L1 cell lines were cultured in Dulbecco's modified Eagle Medium (DMEM) and Minimum Essential Media (MEM), respectively. Each medium was supplemented with 10% fetal bovine serum (FBS) and 1% penicillin/streptomycin (basal growth mediums). Cells were incubated at 37 °C in 5% CO_2 to 90% confluence. Cellular toxicity of SIM-PPI was evaluated using the 3-(4,5-dimethyl-thiazol-2yl)-2,5-diphenyltetrazoliumbromide (MTT) assay. Briefly, Raw 264.7 and MC3T3-L1 cells were seeded in 96 well plates (1×10^4 cells/well) and treated with various concentrations of SIM-PPi, free SIM (0.01 nM to 1 mM, SIM equivalent), and free PPi (PPi in SIM-PPi equivalent), and then incubated for 24, 48 and 72 hr. Following each time point, 10 μL of MTT reagent were added to each well and further incubated for 4 hr at 37 °C. MTT detergent reagent (100 μL) was added to each well to solubilize deposited formazan, then incubated in the dark at room temperature for 2 hr. The absorbance of each well was recorded at 570 nm using a microplate reader (SpectraMax M2, Molecular Devices, Sunnyvale, CA, USA).

Measurement of LPS-induced cytokine—LPS-induced pro-inflammatory cytokines were measured to investigate whether SIM-PPi retains the anti-inflammatory property of SIM. Raw 264.7 cells were seeded into 24-well plate (2×10^5 cells/well) in 1 mL medium and incubated overnight. The cells were pre-treated with 100 nM SIM or its equivalent SIM-PPi or PPi (PPi in SIM-PPi equivalent) for 1 hr before LPS challenge (1 μg/mL); the cells were then incubated in a 37 °C, 5% CO_2 incubator for 24 hr. Supernatants were collected and centrifuged, then stored at −80 °C until assayed for IL-6 and IL-1β concentrations using ELISA kits according to the manufacturer's protocols (Invitrogen).

Measurement of alkaline phosphatase (ALP) activity—Intracellular ALP was measured using *p*-nitrophenyl phosphate as a substrate to investigate whether SIM-PPi retains the osteoinductive property of SIM. Briefly, MC3T3-L1 cells were seeded in 24-well plates at a density of 4×10^4 cells/well in the basal growth medium. At 80% confluence, 100 nM SIM or its equivalent of SIM-PPi or PPi (PPi in SIM-PPi equivalent) were added to the basal growth medium supplemented with 4 mM inorganic phosphate as a phosphate ions source, and the incubation was continued with medium changed every 72 hr. A negative control group (con-) was cultured in only basal growth medium to observe any spontaneous differentiation. Also, a positive control group (con+) was included and cultured in an osteogenic medium which was composed of basal growth medium, 4 mM inorganic phosphate, and osteoinductive supplements (0.28 mM ascorbic acid and 100 nM dexamethasone). After 3, 7, and 14 days, the culture medium was removed, and cell lysate was prepared according to the assay protocol. The cells were washed twice with ice-cold phosphate buffered saline (PBS) followed by scraping the cells with 100 μl of ice-cold lysis buffer. The cells were homogenized with the lysis buffer and centrifuged at high speed (13,000×g for 3 min); the supernatants were frozen at −20 °C until assayed for the ALP activity using a commercial ALP assay kit (BioVision Incorporated, Milpitas, CA).

Alizarin red S staining and quantification—To visualize calcium deposition by differentiated osteoblasts, MC3T3-L1 cells in a 24-well plate were stained with Alizarin red S (ARS) after 28 days of culture with medium change every 72 hr. Briefly, after washing the cellular monolayer with PBS, cells were fixed with 10% formalin for 30 min at room temperature, washed twice with DI water, and then stained with 2% ARS solution (pH 4.3) at room temperature in the dark for 45 min. Cells were then washed five times with DI water and observed for the presence of calcium deposition as identified by red color presence. ARS staining was quantified using the method described by Gregory CA., et al (25). Briefly, following cells staining and washing, the plate was placed in the freezer overnight to dry samples, and then 0.2 mL of 10% acetic acid in each well was added, and the plate was incubated at room temperature with shaking for 30 min. Cells with acetic acid were then scrapped and collected in a micro-centrifuge tube, and vortexed for 30 seconds, followed by heating for 10 min at 85 °C, and then cooling in an ice bath. After centrifugation at 20,000 ×g for 15 min, supernatants were collected, and adjusted pH to 4.3 with 10% ammonium hydroxide (75 μL). Lastly, each sample (50 μL) was placed in an opaque-walled 96-well plate with clear bottom and absorbance measured at 405 nm using a microplate reader (SpectraMax M2, Molecular Devices, Sunnyvale, CA, USA).

von Kossa staining—To further visualize and confirm the mineralized nodules, cells were stained with von Kossa stain after 28 days in culture with medium change every 72 hr; wherein silver ions replace calcium and react with phosphate under strong light to be seen as metallic silver. Cells were washed and fixed in 10% formalin for 30 min, washed with DI water, and then incubated with 5% silver nitrate solution (RICCA Chemical company) at room temperature under bright light for 45 minutes or until mineral deposits turned black or dark brown. After that, cells were washed 3 times with DI water, followed by incubating with 5% sodium thiosulfate (Alfa Aesar) for 5 min to remove unreacted silver. After washing with ID water five times, wells were photographed and visually examined for calcium deposits.

Evaluation of SIM-PPi's therapeutic efficacy on an experimental periodontitis rat model

Sprague Dawley rats (female, 10-month-old, retired breeders) were purchased from Envigo. The animals were acclimated for one week prior to any experimental procedure. Rats were divided randomly into four groups: experimental periodontitis with saline injection; experimental periodontitis with SIM treatment; experimental periodontitis with PPi treatment; experimental periodontitis with SIM-PPi treatment (Table I). A power analysis was performed to determine the number of animals needed to show a 30% difference in bone area stimulated by simvastatin prodrug compared to a control. This analysis used data from previous studies(26,27). In order to detect a greater than 30% change in bone 80% of the time when testing at the 5% level of significance (assuming normality of the data), at least 5 animals would be needed in each group. Since 8 rats/group was used in a previous study testing the same ligature-induced periodontitis model(20), we used the same animal group size. Silk ligatures were used to induce the experimental periodontitis as previously described(20). Briefly, each rat was anesthetized using a chamber attached to isoflurane vaporizer (1– 4% isoflurane and 100% oxygen), followed by body weight measurement. To maintain anesthesia during experimental procedures, a nose cone (0.5% - 2% isoflurane and 100% oxygen) was applied throughout the entire experimental procedure. Experimental periodontitis was induced in all groups by gently tightening a 4–0 silk ligature around the maxillary 2nd molars in both sides. All animals were monitored and checked weekly to monitor the progression of periodontitis. Post-procedure analgesic (flunixin 2.5 mg/kg, *s.c.* every 12 hr) was given when signs of pain were observed. After 2 weeks, ligatures were removed. Different treatments including SIM-PPi (dissolved in 25% isopropyl alcohol as described in the HA binding study, 2.56 mg, equivalent to 1.5mg SIM), SIM acid (dissolved in PBS, 1.56 mg, equivalent to 1.5 mg of SIM), and PPi (dissolved in PBS, 0.26 mg, equivalent to the PPi content in SIM-PPi) were locally injected (10μL) into the palatal gingiva between the maxillary first molar (M1) and second molar (M2) on the first day of week 1, 2 and 3 after ligature placement. In the treatment of human periodontitis, this local delivery would be accompanied by scaling and root planing, but lack of long-term root contamination imprecise root planing with the rat model have led to its omission in most recent local drug-delivery studies(28–30). At week 4, all animals were euthanized using CO_2 asphyxiation followed by dissecting the entire palate including all three molars and placed in 10% formalin for μ-CT and histological evaluations. All animal procedures were approved by the Institutional Animal Care and Use Committee of University of Nebraska Medical Center.

Micro-computed tomography (μ-CT) analysis

At the end-point, palates including all three molars on both sides were collected and fixed in 10% formalin. All samples were scanned using a micro-CT imaging system (Bruker SkyScan1172, Kontich, Belgium), as described in previous studies (20,21). The voltage and current of X-ray source were set at 70 kV and 141 μA, respectively, with a pixel size of 8.6 μm and a 0.5 mm-thick aluminum filter was used. The exposure time was 580 ms, and X-ray projections were obtained at 0.7° intervals with a scanning angular rotation of 180°, and 8 frames were averaged for each rotation. To generate three-dimensional (3D) images, scans were reconstructed using the system-reconstruction software (NRecon; Skyscan). Sagittal sections were obtained using the Skyscan DataViewer software, then the linear distance from the cementoenamel junction (CEJ) to the alveolar bone crest (ABC) was measured in millimeters using the Skyscan CT-Analyzer software. For each sample, the linear distance was measured from two points: distopalatal of M1 and mesiopalatal of M2. Longer distance means more bone loss and vice versa. Coronal sections obtained using the Skyscan DataViewer were used to measure bone volume (BV), trabecular thickness (Tb.Th), trabecular number (Tb.N) and trabecular separation (Tb.Sp) using the CT Analyzer. A rectangular region of interest (ROI, excluding the roots) was selected, with its length extended from the distopalatal of M1 to the mesiopalatal of M2, width from the palatal side to the midline of M1 and M2, and height 130 slices below CEJ of M1 and M2. The sample analysis was performed by two examiners (YA and XBW) independently to ensure accurate assessment.

Histological evaluation

After completing the μ-CT analysis, all specimens were decalcified in 14% ethylenediaminetetraacetic acid (EDTA) solution for one month. After decalcification, samples were embedded in paraffin. Sagittal sections (5μm) were obtained in a mesiodistal direction with roots aligned in one plane and then stained with hematoxylin and eosin for microscopic observation. To evaluate connective tissues between M1 and M2 for inflammatory cell infiltrate and alveolar crest for osteoclasts, a pathologist (SML) who was blind to experimental group arrangement qualitatively assessed samples using a light microscope (Olympus System Microscope Model BX53) under 200× magnification. Neutrophils and lymphocytic infiltrate were evaluated qualitatively in the gingival tissues above the alveolar crest using a scoring system(31,32) (Table II). Osteoclasts lining the surface of alveolar crest were also qualitative assessed using a scoring system(33) (Table III). To calibrate SML's scoring, another researcher (YA) independently scored a stack of slides and compared with SML's results before SML proceeded with all the analyses.

Statistical analysis

All the obtained data were presented as the mean ± standard deviation (SD). Statistical analysis was performed using SPSS 22.0 software (SPSS Inc., Chicago, IL, USA) and Prism 7.0 software (GraphPad, San Diego, CA). Continous outcomes among more than three groups were compared using the one-way Analysis of Variance (ANOVA) for one variable data and two-way ANOVA for two variable data. Tukey's post-hoc multiple comparisons

was conducted in case a significant difference among the group means was found. *P*-value < 0.05 was considered statistically significant.

RESULTS

Aqueous solubility of SIM-PPi

The aqueous solubility of SIM-PPi at 22 ± 2 °C and pH 7 was analyzed and compared to SIM. The solubility of SIM-PPi was determined to be 0.899 mg/mL (equivalent to 0.53 mg/mL of SIM) after being equilibrated for 48 hr in deionized water and 0.969 mg/mL (equivalent to 0.57 mg/mL of SIM) in phosphate buffer. For SIM, its solubility was determined to be 0.0025 mg/mL in deionized water and 0.0073 mg/mL in phosphate buffer. Clearly, conjugating PPi to SIM trimer has greatly improved SIM's water solubility.

SIM-PPi binding to hydroxyapatite (HA)

HA binding assay was performed to assess the bone affinity of SIM-PPi (Fig. 1). After 30 min incubation, SIM-PPi showed significantly higher (23%) binding to HA when compared to SIM alone which did not show any binding. As the HA incubation time extended to 2 hr, SIM-PPi's binding to HA increased to 50% and reached the plateau. After 6 hr of incubation, SIM-PPi's binding to HA remained at 51%. During the entire binding study, SIM exhibited minimum binding to HA. As a strong osteotropic agent and a positive control for the HA binding experiment, ALN showed very strong binding to HA (77%) as expected.

Cell viability

To evaluate the *in vitro* safety of SIM-PPi, both Raw 264.7 and MC3T3-L1 cells were treated with wide range of concentrations of SIM-PPi (1 nM to 1mM, SIM equivalent) for 24, 48 and 72 hr and the cell viability was determined using the MTT assay (Figure 2). For both cell lines, they almost shared the same toxicity profile. The viability of Raw 264.7 cells treated with more than 100 μM of SIM-PPi (SIM equivalent) was substantially decreased over the three days, the viability was less than 60% after 72 hr. The viability of MC3T3-L1 cells treated with more than 250 μM of SIM-PPi (SIM equivalent) was decreased dramatically after three days (less than 40%). However, when both cell lines treated with more than 100 nM of free SIM, the viability was reduced over the three days, indicating that SIM has narrower toxicity range than SIM-PPi. Free PPi increased cell populations and did not show any signs of toxicity for 72 hr. Hence, 100 nM of SIM-PPi (SIM equivalent) was used in the following experiments as non-toxic concentration to evaluate both anti-inflammatory and osteogenic effects on macrophages Raw 264.7 and osteoblasts MC3T3-L1, respectively.

Effect of SIM-PPi on LPS-induced cytokines:

The concentrations of IL-6 and IL-1β were detected in the culture supernatants of Raw 264.7 cells using ELISA kits (Fig. 3). LPS challenged cells showed a tremendous increase in both cytokines comparing to the control group (medium only). SIM-PPi treated group showed a significant reduction in IL-6 ($P < 0.05$) and IL-1β ($P < 0.0001$) when compared to the LPS group. The SIM-treated group exhibited the lowest concentration of both IL-6 and IL-1β.

ALP activity measurement

The ALP activity in the control and experimental groups are shown in Figure 4B. The cells in the negative control culture did not show any significant activity of ALP after 3, 7, and 14 days, as expected. As anticipated, in the positive control culture, the cells expression of ALP was increased significantly over 14 days. Among all the tested samples, free SIM culture showed the highest level of ALP after 3, 7, and 14 days ($P < 0.0001$). At day 7, ALP activity increased significantly for SIM-PPi and PPi cultures compared to the negative control ($P < 0.0001$). After 14 days, SIM-PPi culture continued to express a substantial level of ALP as compared to the negative control ($P < 0.0001$), while PPi culture showed a slight decrease in the ALP activity.

Alizarin red S (ARS) and von Kossa staining

To evaluate calcium deposit and mineralized nodules, ARS and von Kossa staining assays were used. As shown in Figure 4A&C, the two stains showed similar observations, and they were both in agreement with the ALP findings. The negative control group showed very little calcium deposit and ARS quantity, while positive control and SIM treated groups exhibited significant ARS quantity ($P < 0.0001$) with the highest mineralized nodules when compared to negative control (con-), as expected. And most importantly, SIM-PPi treated group showed significantly higher ARS quantity ($P < 0.01$) when compared to negative control and PPi groups, with more mineralized nodules formation. PPi group has the lowest ARS quantity and calcium deposit among all tested groups except the negative control.

Micro-computed tomography (μ-CT) analysis

As shown in Figure 5A, it is obvious that the SIM-PPi treated group preserved alveolar bone crest compared to other treated groups. The linear distance of CEJ to ABC, representing alveolar crest height, indicated that the SIM-PPi treated group had significantly shorter distance when compared to saline-treated group (0.98 mm vs. 1.32 mm, $P > 0.05$). SIM and PPi treated groups did not exhibit statistically significant differences when compared to the saline-treated group as presented in Figure 5B. For further validation of alveolar bone loss, different bone volumetric parameters, as shown in Figure 6, were quantified. The SIM-PPi treated group demonstrated significantly ($P > 0.05$) different values in bone volume (BV, 0.85 mm^3 vs. 0.38 mm^3), trabecular thickness (Tb.Th, 0.78 mm vs. 0.62 mm), trabecular number (Tb.N, 2.86 mm^{-1} vs. 1.69 mm^{-1}) and trabecular separation (Tb.Sp, 0.35 mm vs. 0.47 mm) than the saline group. In contrast, when comparing SIM and PPi treated groups to the saline group, none of the above parameters produced statistically significant differences.

Histological evaluation

To evaluate the effect of the different treatments on the inflammatory infiltrate and osteoclasts, H&E stained sections were assessed qualitatively. Histology scores of neutrophils and lymphocytes were shown in Figure 7B–C, based on the grading criteria in Table II. SIM-PPi treated group earned the lowest score of neutrophils ($P < 0.01$) and lymphocytes ($P < 0.0001$) when compared to saline group, while neutrophils of SIM-treated group did not exhibit statistically significant difference when compared to the saline group.

Osteoclast scores of the SIM-PPi-treated group were the lowest among all the treatment groups and were significantly lower than the saline-treated group (Figure 7D, $P < 0.05$).

DISCUSSION

Simvastatin (SIM) has been reported to have osteogenic (10,11) and anti-inflammatory properties (13,14), making it a promising candidate for therapeutic intervention for periodontal diseases. Local application of SIM has been explored in periodontitis treatment (16,34–36). The lack of osteotropicity and its poor water solubility have limited the clinical applications of SIM in managing periodontitis. To overcome these limitations, alternatives technologies for local delivery of SIM have been developed to enhance solubility and to provide a sustained release; and have shown potential protection of the periodontal tissues. In a previous study, local application of SIM (0.5 mg)/alendronate-β-cyclodextrin complex (SIM–ALN–CD) was tested on a LPS-induced periodontitis as a preventative agent against a future episode of periodontitis. It was concluded that the locally applied SIM–ALN–CD has the potential to prevent periodontitis associated bone loss(21). A concern with this formulation is the use of ALN (a bisphosphonate) as the bone-homing moiety. It has been well recognized that the long-term clinical use of bisphosphonates has been associated with higher incident rates of osteonecrosis of the jaw (ONJ) and atypical fracture (37,38). Another previous study aimed to examine the effect of a locally delivered SIM prodrug in a ligature-induced periodontitis rat model(20). The amphiphilic macromolecular prodrug of SIM (1.5 mg) was designed and prepared by conjugating SIM trimer to a polyethylene glycol monomethylether (mPEG) molecule. The study concluded that three weekly injections of the macromolecular SIM prodrug (SIM-PEG) decreased alveolar bone loss and inflammation in rats. While the SIM-PEG design solubilizes SIM in water by forming micelles, a limitation of this prodrug is its lack of osteotropicity and the relatively low drug loading.

To provide SIM with better water solubility and osteotropicity but also to avoid potential long-term side effects associated with bisphosphonates (e.g. ONJ), we have developed a novel SIM prodrug by conjugating SIM trimer directly to a pyrophosphate (PPi) (Scheme 1). This design was built upon the findings of our previous studies(20,21). The three SIMs are chemically conjugated via ester bonds which can be hydrolyzed *in vivo* in the presence of esterases. One of the three SIMs conjugated to PPi is in the active SIM acid form, and the other two are in the lactone form, which would be activated upon exposure to the *in vivo* environment (e.g. esterase, water, low pH, and elevated temperature). Pyrophosphate (PPi) is a water-soluble and calcium-binding molecule. It is known for decades in the food industry as a leavening agent. Due to its high affinity to enamel, dentin, and tarter (39), it has been used widely in dental and oral care products (40–42). PPi is biodegradable (via phosphatase) with phosphate as its degradation product, which has a much better safety profile than the bisphosphonates (37,38). Therefore, we proposed to conjugate PPi to SIM-trimer to improve SIM's water solubility and to provide osteotropicity. The findings of the present study validate these design objectives and confirm the anti-inflammatory and periodontal bone preservation/regeneration capacity of the SIM-PPi design on an experimental periodontitis rat model.

Conjugating PPi to SIM trimer increased its water solubility over 200-fold. The binding experiment (Figure 1) showed that SIM-PPi has stronger binding to HA than free SIM, confirming that SIM-PPi as a bone-specific prodrug is a viable strategy for local delivery of SIM to the skeletal tissues. In Raw 264.7 culture, SIM-PPi was found to effectively inhibited LPS-induced interleukin-1β (IL-1β), which is considered as one of the most potent inducers of bone resorption, and interleukin-6 (IL-6), which is secreted in response to bone resorbing inducers including IL-1β(43). These findings suggest that SIM-PPi may reduce periodontal inflammation by attenuating the pro-inflammatory cytokines secreted by the inflammatory cells. The data also showed that SIM-PPi could significantly increase ALP activity in MC3T3-E1 culture after 7 and 14 days when compared to negative control (Figure 4B). In addition, ARS and Von Kossa staining data indicated that SIM-PPi significantly increased calcium deposits and mineralized nodules formation in MC3T3-E1 when compared to negative control (Figure 4A&C). Taken together, these *in vitro* data confirm that SIM-PPi retains the well-established SIM-mediated anti-inflammatory (13,14) and osteoinductive (44) activities after conjugating with PPi. It is important to note that due to its prodrug nature (needs to be activated to be therapeutically effective), SIM-PPi showed lower *in vitro* activity than SIM.

When evaluated *in vivo* using a ligature-induced periodontitis rat model, micro-CT analysis of alveolar bone showed that the SIM-PPi treatment was the most effective treatment among all groups in preserving alveolar bone integrity (Figures 5&6). It significantly prevented alveolar crest loss (Figure 5) and maintained bone volumetric parameters (BV, Tb.Th, Tb.N, and Tb.Sp) (Figure 6) when compared to saline control. Also, in accordance with the micro-CT findings, histological evaluation revealed a superior anti-inflammatory effect of SIM-PPi. It significantly reduced both inflammatory cell infiltrate (neutrophil and lymphocyte) and osteoclast score when compared to control (Figure 7). PPi itself did not show any significant protective effects against bone loss indicating that it did not contribute to preserving alveolar bone integrity. Ideally, a local treatment for periodontal bone loss should be given when developing periodontitis lesions are identified. Therefore, to make the treatment more clinically relevant, the weekly SIM-PPi injections was initiated at the time of ligature placement and continued for 3 weeks.

Overall, the weekly administration of SIM-PPi was found to be more effective in preventing periodontitis-induced alveolar bone loss when compared to dose equivalent SIM treatment. We believe that SIM-PPi's retention after local administration in combination with its gradual activation and releasing of simvastatin acid provide a rational explanation of the superior therapeutic effect of SIM-PPi over free SIM in prevention of alveolar bone loss associated with periodontitis. Furthermore, the weekly SIM-PPi administration schedule, possibly using pocket irrigation, would be easily adapted into current dental preventive care practice, indicative of a high clinical translation potential.

CONCLUSION

In this study, we report the design and synthesis of a novel osteotropic simvastatin (SIM) prodrug by conjugating three SIMs to a pyrophosphate (PPi). This prodrug design not only enhanced SIM solubility but also exhibited affinity to hydroxyapatite (HA), with retained

bone anabolic and anti-inflammatory properties of SIM. When tested on an experimental periodontitis rat model, SIM-PPi was found to be effective in preserving periodontal bone. Upon further optimization, we believe this novel simvastatin prodrug may have the potential to be developed into a novel clinical management of periodontal diseases.

ACKNOWLEDGEMENT

This work was financially supported in part by a grant from National Institute of Health (R01 AI119090) and the University of Nebraska Medical Center College of Pharmacy. Yosif Almoshari was supported by the Ministry of Education Scholarship, Jazan University (Jazan, Saudi Arabia). The content is solely the responsibility of the authors and does not necessarily represent the official views of the National Institutes of Health. DW, RAR, XBW and ZSJ are co-inventors of a patent application of the SIM-PPi prodrug technology. The other authors report no conflicts of interest related to this study.

ABBREVIATIONS

ABC	Alveolar bone crest
ALP	Alkaline phosphatase
BMP-2	Bone morphogenetic protein-2
CEJ	Cementoenamel junction
EDTA	Ethylenediaminetetraacetic acid
GCF	Gingival crevicular fluid
HA	Hydroxyapatite
HMG-CoA	3-Hydroxy-3-methyl-glutaryl-coenzyme A
LPS	Lipopolysaccharide
M1	First molar
M2	Second molar
MCP-1	Monocyte chemoattractant protein-1
MMPs	Matrix metalloproteinases
MTT	3-(4,5-Dimethyl- thiazol-2yl)-2,5- diphenyltetrazoliumbromide
OPG	Osteoprotegerin
PPi	Pyrophosphate
RANK	Receptor activator of nuclear factor-kappa B
RANKL	Receptor activator of nuclear factor-kappa B ligand
ROI	Region of interest
SIM	Simvastatin

SIM-PPi	Simvastatin-pyrophosphate
Tb.N	Trabecular number
Tb.Sp	Trabecular spacing or separation
Tb.Th	Trabecular thickness
μ-CT	Micro-computed tomography

REFERENCES:

1. Pihlstrom BL, Michalowicz BS, Johnson NW. Periodontal diseases. Lancet [Internet]. 2005 11 19 [cited 2017 Nov 6];366(9499):1809–20. Available from: http://www.ncbi.nlm.nih.gov/pubmed/16298220
2. Eke PI, Dye BA, Wei L, Slade GD, Thornton-Evans GO, Borgnakke WS, et al. Update on Prevalence of Periodontitis in Adults in the United States: NHANES 2009 to 2012. J Periodontol [Internet]. 2015 5 [cited 2017 Dec 22];86(5):611–22. Available from: http://www.ncbi.nlm.nih.gov/pubmed/25688694
3. Hajishengallis G Periodontitis: from microbial immune subversion to systemic inflammation. Nat Rev Immunol [Internet]. 2014;15(1):30–44. Available from: http://www.ncbi.nlm.nih.gov/pubmed/25534621
4. Krayer JW, Leite RS, Kirkwood KL. Non-surgical chemotherapeutic treatment strategies for the management of periodontal diseases. Dent Clin North Am [Internet]. 2010 1 [cited 2017 Aug 23];54(1):13–33. Available from: http://www.ncbi.nlm.nih.gov/pubmed/20103470
5. Herrera D, Sanz M, Jepsen S, Needleman I, Roldán S. A systematic review on the effect of systemic antimicrobials as an adjunct to scaling and root planing in periodontitis patients. J Clin Periodontol [Internet]. 2002 [cited 2017 Aug 23];29 Suppl 3:136–59; discussion 160–2. Available from: http://www.ncbi.nlm.nih.gov/pubmed/12787214
6. Greenstein G Local drug delivery in the treatment of periodontal diseases: assessing the clinical significance of the results. J Periodontol [Internet]. 2006 4 [cited 2017 Aug 23];77(4):565–78. Available from: http://www.joponline.org/doi/10.1902/jop.2006.050140
7. Williams RC, Jeffcoat MK, Howell TH, Reddy MS, Johnson HG, Hall CM, et al. Ibuprofen: An inhibitor of alveolar bone resorption in beagles. J Periodontal Res [Internet]. 1988 7 1 [cited 2017 Aug 23];23(4):225–9. Available from: http://doi.wiley.com/10.1111/j.1600-0765.1988.tb01363.x
8. Raja S, Byakod G, Pudakalkatti P. Growth factors in periodontal regeneration. Int J Dent Hyg [Internet]. 2009 5 [cited 2017 Aug 23];7(2):82–9. Available from: http://www.ncbi.nlm.nih.gov/pubmed/19413545
9. Bellosta S, Bernini F, Ferri N, Quarato P, Canavesi M, Arnaboldi L, et al. Direct vascular effects of HMG-CoA reductase inhibitors. Atherosclerosis [Internet]. 1998 4 [cited 2017 Aug 23];137 Suppl:S101–9. Available from: http://www.ncbi.nlm.nih.gov/pubmed/9694549
10. Mundy G, Garrett R, Harris S, Chan J, Chen D, Rossini G, et al. Stimulation of bone formation in vitro and in rodents by statins. Science [Internet]. 1999;286(5446):1946–9. Available from: http://www.ncbi.nlm.nih.gov/pubmed/10583956
11. Garrett IR, Mundy GR. The role of statins as potential targets for bone formation. Arthritis Res [Internet]. 2002 [cited 2017 Aug 23];4(4):237 Available from: http://www.ncbi.nlm.nih.gov/pubmed/12106493
12. Emani S, Gunjiganur G, Mehta D. Determination of the antibacterial activity of simvastatin against periodontal pathogens, Porphyromonas gingivalis and Aggregatibacter actinomycetemcomitans: An in vitro study. Contemp Clin Dent [Internet]. 2014 7 [cited 2017 Apr 27];5(3):377 Available from: http://www.ncbi.nlm.nih.gov/pubmed/25191077
13. Lazzerini PE, Lorenzini S, Selvi E, Capecchi PL, Chindamo D, Bisogno S, et al. Simvastatin inhibits cytokine production and nuclear factor-kB activation in interleukin 1??-stimulated synoviocytes from rheumatoid arthritis patients. Clin Exp Rheumatol. 2007;25(5):696–700. [PubMed: 18078616]

14. Pereira MC, Cardoso PRG, Da Rocha LF, Rêgo MJBM, Gonçalves SMC, Santos FA, et al. Simvastatin inhibits cytokines in a dose response in patients with rheumatoid arthritis. Inflamm Res. 2014;63(4):309–15. [PubMed: 24419251]
15. Cunha-Cruz J, Saver B, Maupome G, Hujoel PP. Statin Use and Tooth Loss in Chronic Periodontitis Patients. J Periodontol [Internet]. 2006 6 [cited 2017 Nov 5];77(6):1061–6. Available from: http://www.ncbi.nlm.nih.gov/pubmed/16734582
16. Pradeep AR, Thorat MS. Clinical Effect of Subgingivally Delivered Simvastatin in the Treatment of Patients With Chronic Periodontitis: A Randomized Clinical Trial. J Periodontol [Internet]. 2010 2 [cited 2017 Nov 6];81(2):214–22. Available from: http://www.ncbi.nlm.nih.gov/pubmed/20151799
17. Agarwal S, Chaubey K, Chaubey A, Agarwal V, Madan E, Agarwal M. Clinical efficacy of subgingivally delivered simvastatin gel in chronic periodontitis patients. J Indian Soc Periodontol [Internet]. 2016 [cited 2018 May 25];20(4):409 Available from: http://www.ncbi.nlm.nih.gov/pubmed/28298823
18. Priyanka N, Abhilash A, Saquib S, Malgaonkar N, Kudyar N, Gupta A, et al. Clinical Efficacy of Subgingivally Delivered 1.2 mg Simvastatin in the Treatment of Patients with Aggressive Periodontitis: A Randomized Controlled Clinical Trial. Int J Periodontics Restorative Dent [Internet]. [cited 2018 May 25];37(2):e135–41. Available from: http://www.ncbi.nlm.nih.gov/pubmed/28196160
19. Akram Z, Vohra F, Javed F. Efficacy of statin delivery as an adjunct to scaling and root planing in the treatment of chronic periodontitis: A meta-analysis. J Investig Clin Dent [Internet]. 2018 5 [cited 2018 May 25];9(2):e12304 Available from: http://www.ncbi.nlm.nih.gov/pubmed/29119729
20. Bradley AD, Zhang Y, Jia Z, Zhao G, Wang X, Pranke L, et al. Effect of Simvastatin Prodrug on Experimental Periodontitis. J Periodontol [Internet]. 2016 5 [cited 2017 Apr 2];87(5):577–82. Available from: http://www.ncbi.nlm.nih.gov/pubmed/26799395
21. Price U, Le HOT, Powell SE, Schmid MJ, Marx DB, Zhang Y, et al. Effects of local simvastatin-alendronate conjugate in preventing periodontitis bone loss. J Periodontal Res. 2013;48(5):541–8. [PubMed: 23278592]
22. He Y, Ho C, Yang D, Chen J, Orton E. Measurement and Accurate Interpretation of the Solubility of Pharmaceutical Salts. J Pharm Sci [Internet]. 2017 5 [cited 2018 Jan 15];106(5):1190–6. Available from: http://linkinghub.elsevier.com/retrieve/pii/S0022354917300266
23. Serajuddin AT, Ranadive SA, Mahoney EM. Relative lipophilicities, solubilities, and structure-pharmacological considerations of 3-hydroxy-3-methylglutaryl-coenzyme A (HMG-CoA) reductase inhibitors pravastatin, lovastatin, mevastatin, and simvastatin. J Pharm Sci [Internet]. 1991 9 [cited 2018 Jan 17];80(9):830–4. Available from: http://www.ncbi.nlm.nih.gov/pubmed/1800703
24. Taha EA, Youssef NF. Spectrophotometric determination of some drugs for osteoporosis. Chem Pharm Bull (Tokyo) [Internet]. 2003 12 [cited 2018 May 25];51(12):1444–7. Available from: http://www.ncbi.nlm.nih.gov/pubmed/14646329
25. Gregory CA, Gunn WG, Peister A, Prockop DJ. An Alizarin red-based assay of mineralization by adherent cells in culture: comparison with cetylpyridinium chloride extraction. Anal Biochem [Internet]. 2004 6 1 [cited 2017 Nov 16];329(1):77–84. Available from: http://linkinghub.elsevier.com/retrieve/pii/S0003269704001332
26. Stein D, Lee Y, Schmid MJ, Killpack B, Genrich MA, Narayana N, et al. Local simvastatin effects on mandibular bone growth and inflammation. J Periodontol [Internet]. 2005 11 [cited 2018 Jun 1];76(11):1861–70. Available from: http://www.ncbi.nlm.nih.gov/pubmed/16274305
27. Lee Y, Schmid MJ, Marx DB, Beatty MW, Cullen DM, Collins ME, et al. The effect of local simvastatin delivery strategies on mandibular bone formation in vivo. Biomaterials [Internet]. 2008 4 [cited 2018 Jun 1];29(12):1940–9. Available from: http://www.ncbi.nlm.nih.gov/pubmed/18255137
28. Nunes NLT, Messora MR, Oliveira LF, Lisboa M, Barcellos Garcia MC, Rêgo ROCC, et al. Effects of Local Administration of Tiludronic Acid on Experimental Periodontitis in Diabetic Rats. J Periodontol [Internet]. 2017 9 15 [cited 2018 May 25];1–19. Available from: http://www.ncbi.nlm.nih.gov/pubmed/28914593

29. Camacho-Alonso F, Davia-Peña RS, Vilaplana-Vivo C, Tudela-Mulero MR, Merino JJ, Martínez-Beneyto Y. Synergistic effect of photodynamic therapy and alendronate on alveolar bone loss in rats with ligature-induced periodontitis. J Periodontal Res [Internet]. 2018 6 [cited 2018 May 25];53(3):306–14. Available from: http://www.ncbi.nlm.nih.gov/pubmed/29086417
30. Wada-Mihara C, Seto H, Ohba H, Tokunaga K, Kido J, Nagata T, et al. Local administration of calcitonin inhibits alveolar bone loss in an experimental periodontitis in rats. Biomed Pharmacother [Internet]. 2018 1 [cited 2018 May 25];97:765–70. Available from: http://www.ncbi.nlm.nih.gov/pubmed/29107933
31. Gibson-Corley KN, Olivier AK, Meyerholz DK. Principles for Valid Histopathologic Scoring in Research. Vet Pathol [Internet]. 2013 11 4 [cited 2018 May 23];50(6):1007–15. Available from: http://www.ncbi.nlm.nih.gov/pubmed/23558974
32. Schett G, Stolina M, Bolon B, Middleton S, Adlam M, Brown H, et al. Analysis of the Kinetics of Osteoclastogenesis in Arthritic Rats. ARTHRITIS Rheum [Internet]. 2005 [cited 2018 May 25];52(10):3192–201. Available from: https://onlinelibrary.wiley.com/doi/pdf/10.1002/art.21343
33. Bolon B, Morony S, Cheng Y, Hu Y-L, Feige U. Osteoclast Numbers in Lewis Rats with Adjuvant-induced Arthritis: Identification of Preferred Sites and Parameters for Rapid Quantitative Analysis 1. Vet Pathol [Internet]. 2004 [cited 2018 May 25];41:30–6. Available from: http://journals.sagepub.com/doi/pdf/10.1354/vp.41-1-30
34. Vaziri H, Naserhojjati-Roodsari R, Tahsili-Fahadan N, Khojasteh A, Mashhadi-Abbas F, Eslami B, et al. Effect of Simvastatin Administration on Periodontitis-Associated Bone Loss in Ovariectomized Rats. J Periodontol [Internet]. 2007 8 [cited 2017 Nov 6];78(8):1561–7. Available from: http://www.ncbi.nlm.nih.gov/pubmed/17668976
35. Xu X-C, Chen H, Zhang X, Zhai Z-J, Liu X-Q, Qin A, et al. Simvastatin prevents alveolar bone loss in an experimental rat model of periodontitis after ovariectomy. J Transl Med [Internet]. 2014;12:284 Available from: http://www.pubmedcentral.nih.gov/articlerender.fcgi?artid=4192445&tool=pmcentrez&rendertype=abstract
36. Elavarasu S, Suthanthiran TK, Naveen D. Statins: A new era in local drug delivery. J Pharm Bioallied Sci [Internet]. 2012 8 [cited 2017 Nov 6];4(Suppl 2):S248–51. Available from: http://www.ncbi.nlm.nih.gov/pubmed/23066263
37. Durie BGM, Katz M, Crowley J. Osteonecrosis of the Jaw and Bisphosphonates. N Engl J Med [Internet]. 2005 7 7 [cited 2017 Nov 6];353(1):99–102. Available from: http://www.ncbi.nlm.nih.gov/pubmed/16000365
38. Kennel KA, Drake MT. Adverse effects of bisphosphonates: implications for osteoporosis management. Mayo Clin Proc [Internet]. 2009 7 [cited 2017 Nov 6];84(7):632–7; quiz 638. Available from: http://www.ncbi.nlm.nih.gov/pubmed/19567717
39. Shellis RP, Addy M, Rees GD. In vitro studies on the effect of sodium tripolyphosphate on the interactions of stain and salivary protein with hydroxyapatite. J Dent [Internet]. 2005 4 [cited 2017 Nov 6];33(4):313–24. Available from: http://www.ncbi.nlm.nih.gov/pubmed/15781139
40. Hefferren JJ. Historical view of dentifrice functionality methods. J Clin Dent [Internet]. 1998 [cited 2017 Nov 6];9(3):53–6. Available from: http://www.ncbi.nlm.nih.gov/pubmed/10518861
41. Joiner A Whitening toothpastes: A review of the literature. J Dent [Internet]. 2010 1 [cited 2017 Nov 6];38:e17–24. Available from: http://www.ncbi.nlm.nih.gov/pubmed/20562012
42. Yankell SL, Emling RC, Petrone ME, Rustogi K, Volpe AR, DeVizio W, et al. A six-week clinical efficacy study of four commercially available dentifrices for the removal of extrinsic tooth stain. J Clin Dent [Internet]. 1999 [cited 2017 Nov 6];10(3 Spec No):115–8. Available from: http://www.ncbi.nlm.nih.gov/pubmed/10825858
43. Yucel-Lindberg T, Båge T. Inflammatory mediators in the pathogenesis of periodontitis. Expert Rev Mol Med [Internet]. 2013;15(August):e7 Available from: http://www.ncbi.nlm.nih.gov/pubmed/23915822
44. Pagkalos J, Cha JM, Kang Y, Heliotis M, Tsiridis E, Mantalaris A. Simvastatin induces osteogenic differentiation of murine embryonic stem cells. J Bone Miner Res [Internet]. 2010 11 [cited 2017 Nov 16];25(11):2470–8. Available from: http://doi.wiley.com/10.1002/jbmr.163

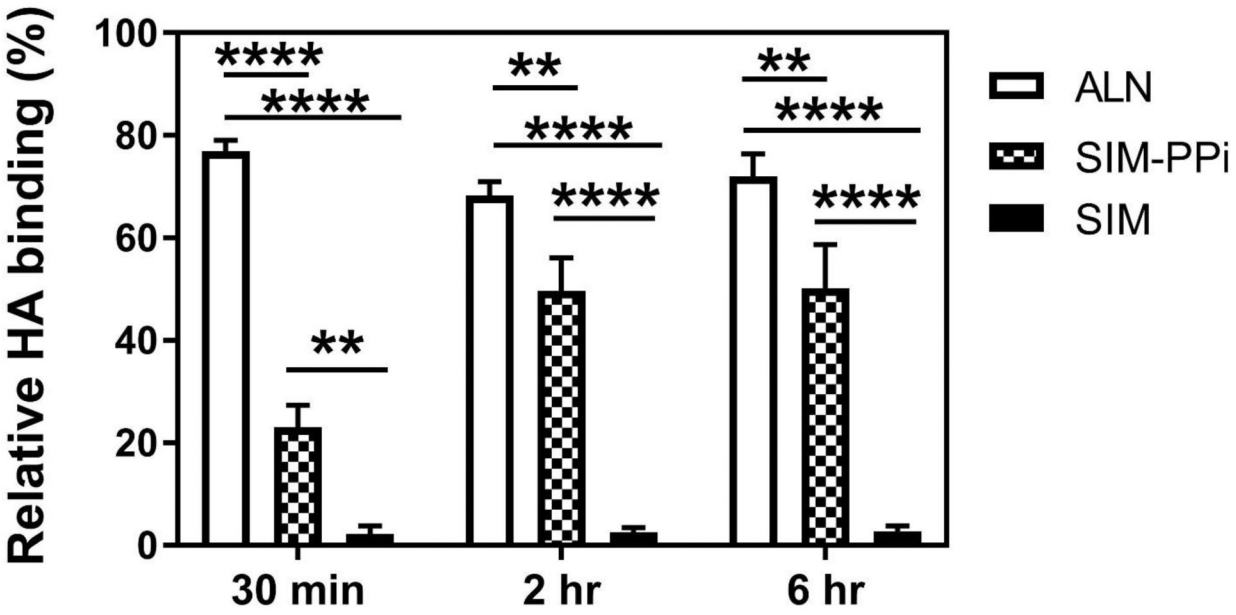

Figure 1.

Quantitative assessment of hydroxyapatite (HA) binding of SIM-PPi with varying length of incubation time: 0.5, 2, and 6 hr. Alendronate (ALN) and free simvastatin (SIM) were used as a positive and negative controls, respectively. *p<0.05, **p< 0.01, and ****p<0.0001 (two-way ANOVA with Tukey's multiple comparisons).

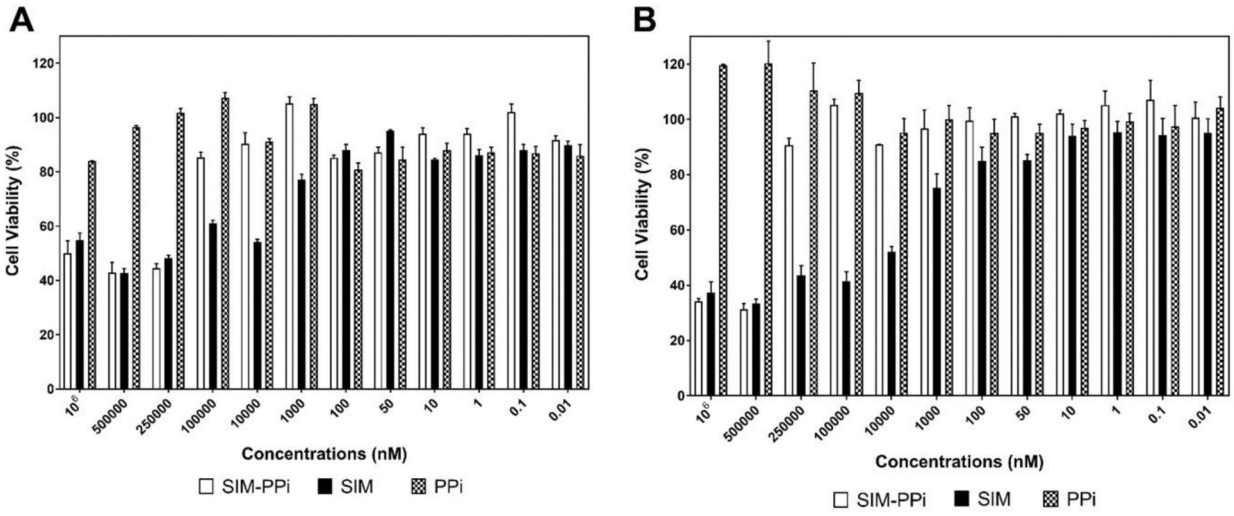

Figure 2.

Effect of different concentrations of SIM-PPi, SIM, and PPi on growth of **(A)** Raw 264.7 cells and **(B)** MC3T3-E1 cells measured by MTT assay following 72-hour exposure. Data are shown as the mean ± SD.

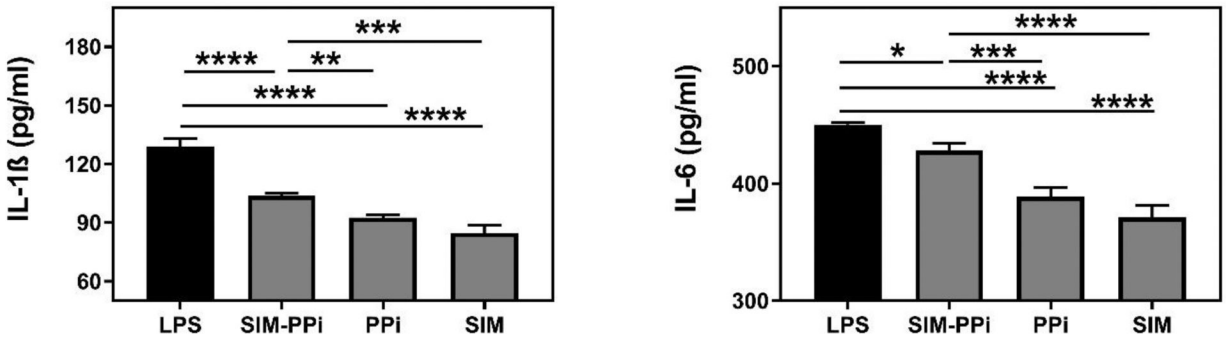

Figure 3.

The impact of SIM (100 nM), PPi, and SIM-PPi (equivalent dose) on LPS-induced IL-1β and IL-6 secretion in Raw 264.7 cells. Mean cytokine concentrations are shown ± SD. *p< 0.05, **p< 0.01, ***p<0.001, and ****p< 0.0001 (one-way ANOVA with Tukey's multiple comparisons).

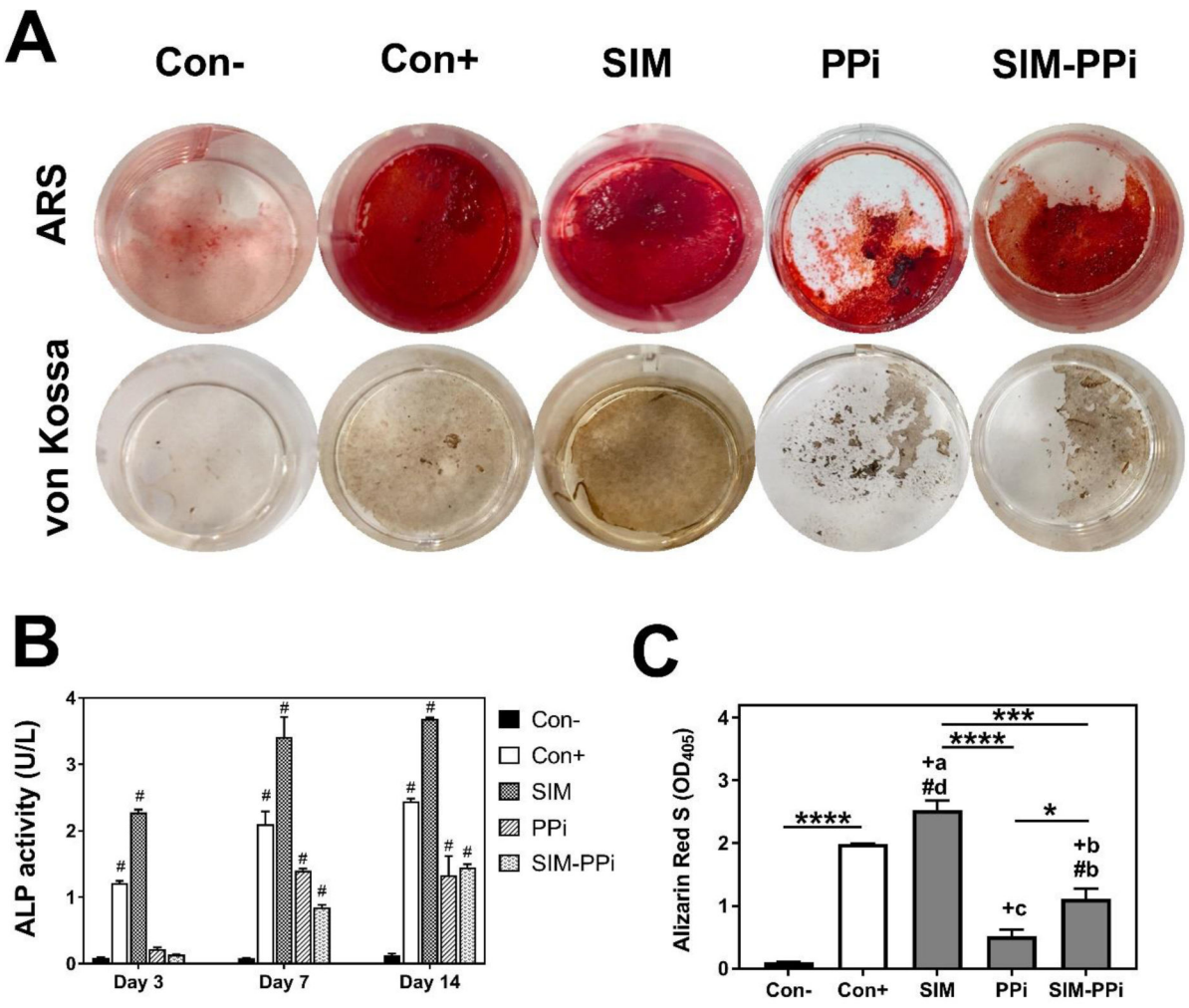

Figure 4.

The *in vitro* evaluation of SIM-PPi's osteogenic efficacy using MC3T3-E1 cell line. **(A)** Representative images of Alizarin Red S **(**ARS) and von Kossa stained wells after 28 days of culture in a 24-well plate with SIM, PPi, and SIM-PPi treatments. **(B)** Alkaline phosphatase (ALP) activity of MC3T3-E1 cell line treated with 100 nM dose equivalent of SIM, PPi, and SIM-PPi. ALP was measured after 3, 7, and 14 days of culture. The values are shown as mean ± SD. $^{\#}p< 0.0001$ when compared to negative control (two-way ANOVA with Dunnett's multiple comparisons). **(C)** ARS quantification measured at 405 nm. $^{*}p<0.05$, $^{***}p<0.001$, $^{****}p<0.0001$. $^{\#b}p<0.01$ and $^{\#d}p<0.0001$ when compared to negative control group. $^{+a}p<0.05$, $^{+b}p<0.01$, and $^{+c}p<0.001$ when compared to positive control group (one-way ANOVA with Tukey's multiple comparisons).

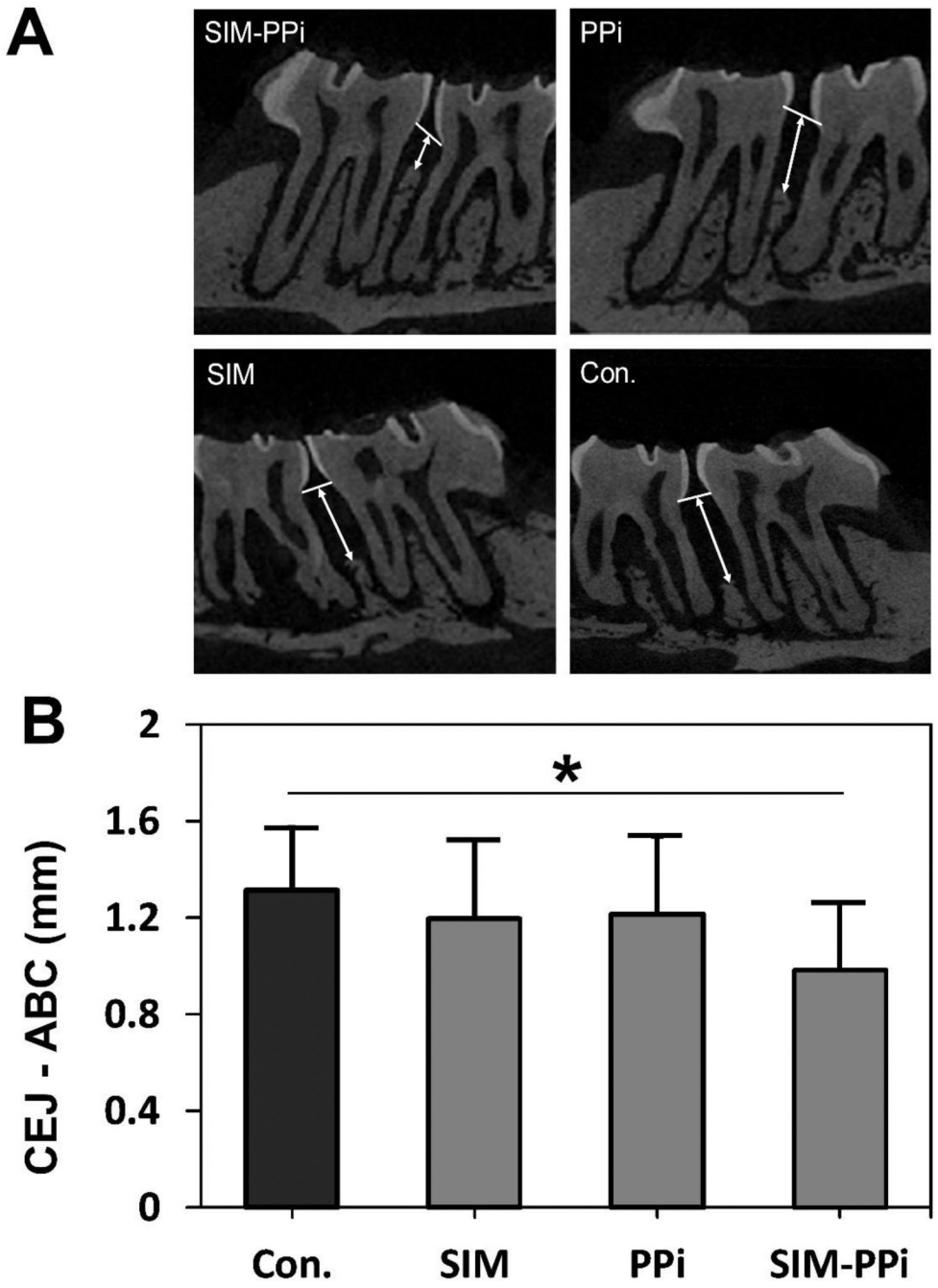

Figure 5.

The *in vivo* evaluation of SIM-PPi efficacy in experimental periodontitis rat model. **(A)** Micro-CT sagittal images showing the effect of different treatments on the maxilla of cementoenamel junction (CEJ) to alveolar bone crest (ABC). White arrows indicate ABC-CEJ distance. **(B)** Measurement of the linear distance between cementoenamel junction (CEJ) and alveolar bone crest (ABC). Values are presented as the mean ± SD. *$p < 0.05$ (one-way ANOVA with Tukey's multiple comparisons).

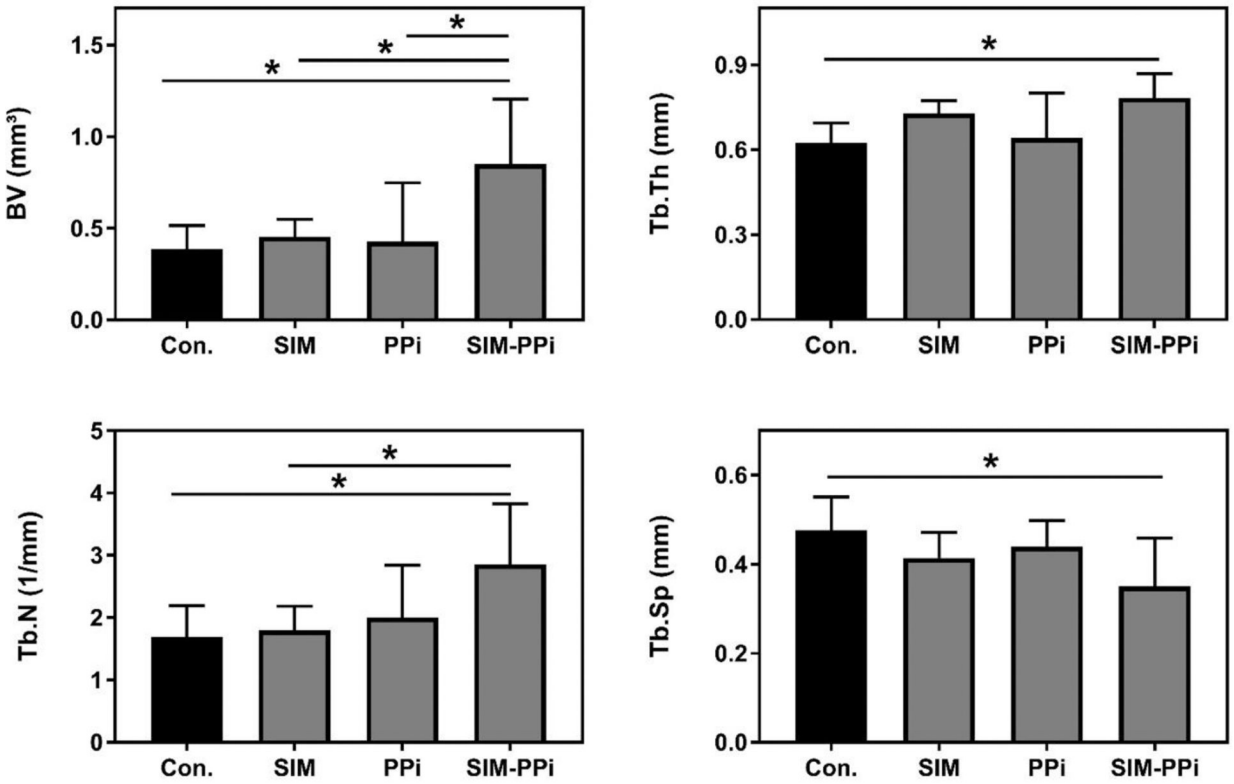

Figure 6.

Micro-CT analysis of alveolar bone quality after different treatments. Bone volume (BV), trabecular thickness (Tb.Th), trabecular number (Th.N), and trabecular separation (Tb.Sp). Values are presented as the mean ± SD. *$p < 0.05$ (one-way ANOVA with Tukey's multiple comparisons).

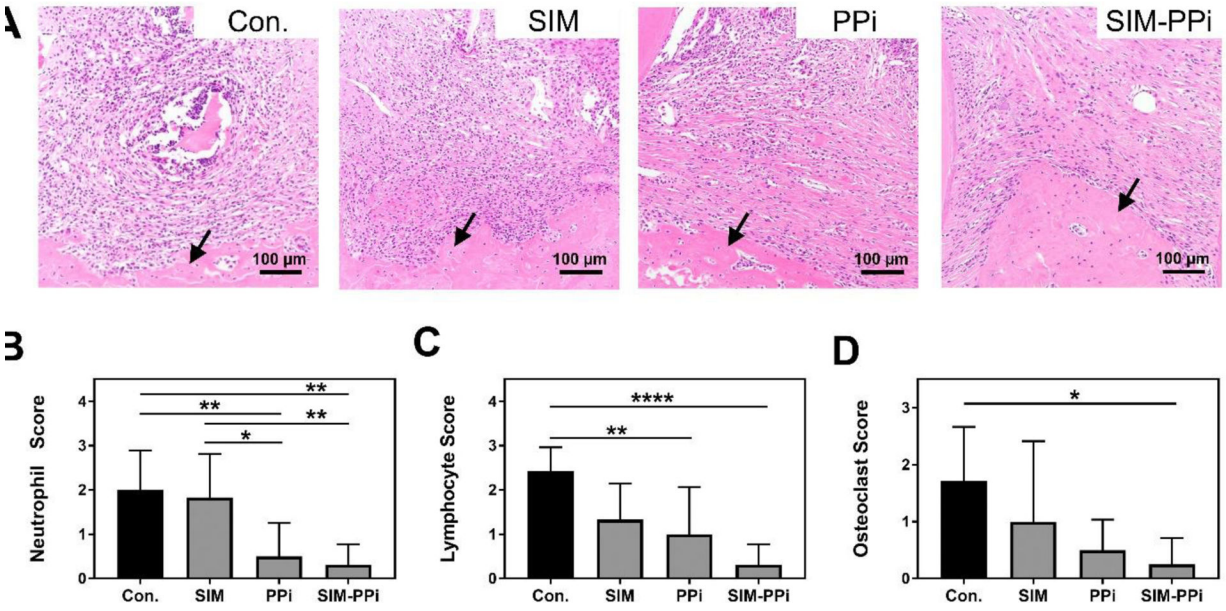

Figure 7.

Histological analysis of papillary connective tissue and alveolar bone between first molar (M1) and second molar (M2) after 3 weeks of different treatments. **(A)** Representative images from different treatment groups of H&E stained sections of connective tissue above the alveolar bone crest (ABC) and between first molar (M1) and second molar (M2). Black arrows indicate alveolar bone crest. **(B-C)** Qualitative assessment of neutrophil and lymphocytic infiltrate interproximally between first molar (M1) and second molar (M2). Scoring criteria is shown in Table II, *p< 0.05, **p< 0.01, and ****p<0.0001 (one-way ANOVA). **(D)** Qualitative assessment of osteoclasts lining the surface of alveolar bone crest. Scoring criteria is shown in Table III, *p< 0.05 (one-way ANOVA with Tukey's multiple comparisons).

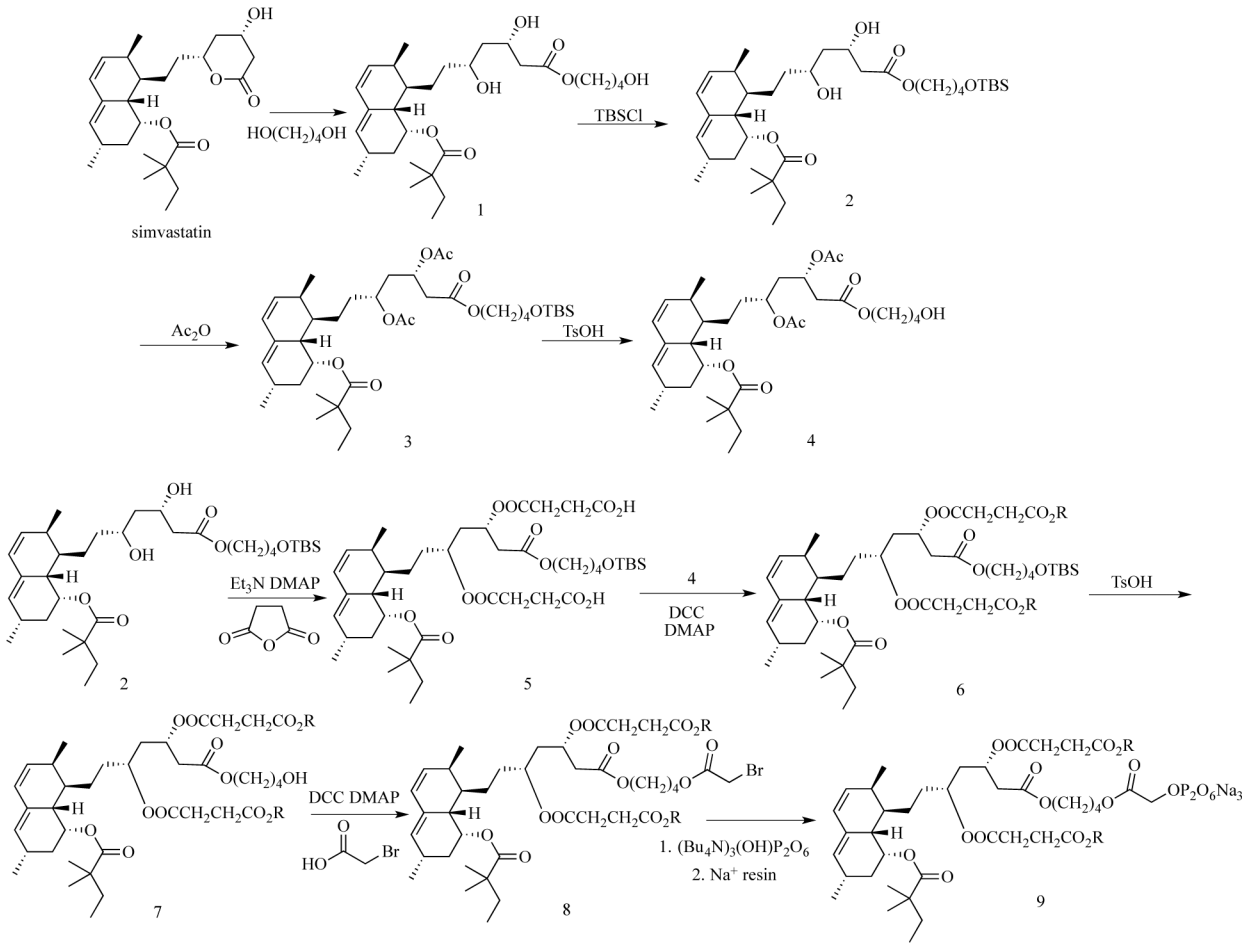

Scheme 1.

The synthesis of simvastatin trimer pyrophosphate prodrug (SIM-PPi).

Table I.

In vivo experimental design.

Group	Number	Side	Week 1*	Week 2*	Week 3*	Week 4
1	8	Left	Ligatures, SIM-PPi	SIM-PPi	Remove Ligatures, SIM-PPi	Euthanized
		Right	Ligatures, PPi	PPi	Remove Ligatures, PPi	Euthanized
2	8	Left	Ligatures, SIM	SIM	Remove Ligatures, SIM	Euthanized
		Right	Ligatures, Saline	Saline	Remove Ligatures, Saline	Euthanized

* Doses: SIM-PPi (2.56 mg, equiv. 1.5mg SIM), SIM acid (1.56mg, equiv. 1.5mg SIM), PPi (0.26 mg equivalent to PPi content in SIM-PPi). (10 μL injection volume).

Table II.

Description of histological scores of neutrophils and lymphocytes.

Score	Evaluation
0	Normal (no inflammatory cells).
1	Few inflammatory cells (lining < 30 % of the affected tissues above the alveolar crest and between M1 & M2).
2	Some inflammatory cells (lining 30 – 60 % of the affected tissues above the alveolar crest and between M1 & M2).
3	Many inflammatory cells (lining > 60 % of the affected tissues above the alveolar crest and between M1 & M2).

Table III.

Description of histological scores of osteoclasts.

Score	Evaluation
0	Normal (no osteoclasts).
1	Few osteoclasts (lining < 5% of most affected alveolar bone surface).
2	Some osteoclasts (lining 5 – 25% of most affected alveolar bone surface).
3	Many osteoclasts (lining 25 – 50% of most affected alveolar bone surface).